LONG-TERM EXPERIENCE OF THE THERMO-ACTIVE GROUND SOURCE SYSTEM AT THE METRO STATION TABORSTRASSE IN VIENNA

Dietmar Adam[*,†], Adrian Brunner[†], Roman Markiewicz,
Johannes Pistrol

TU Wien, Institute of Geotechnics, Karlsplatz 13/220, A-1040 Vienna, Austria

[*] corresponding author: `dietmar.adam@tuwien.ac.at`

[†] shared first authorship

Abstract. Four of the stations newly opened during the underground extension of the U2 line in Vienna in 2008 have been covering a large part of their heating and cooling needs for now almost one and a half decades by using geothermal energy, which is generated by means of energy diaphragm walls, energy piles and energy bottom slabs of the station buildings. As this was the first infrastructure building of this type and scale worldwide at the time of construction, one of the diaphragm walls of the Taborstraße station was equipped with numerous sensors to obtain data sets for the thermo-mechanical long-term behavior of these wall elements for the very first time. Continuous measurements with automatic data recording were initially carried out from April 2008 until May 2011. In October 2020, the measurements were resumed with the existing sensors, this time manually and once a month, in order to carry out a long-term comparison of the measurement data and to create a basis for assessing the effects of the geothermal operation on its structural components. This paper gives an overview of the Taborstraße station with a focus on the thermally activated geostructures and their instrumentation. A comparison of the recorded generated energy with the predicted heating and cooling demand is discussed in the context of the energy data. In addition, the temperature and the strain behavior of the observed energy diaphragm wall is discussed based on the measurement data collected over a period of around 14 years of operational experience.

Keywords: Environmental geotechnics, renewable energy, geothermal energy, energy geo-structures.

1. Introduction

1.1. Reasons for the use of geothermal energy

The use of near-surface geothermal energy has become increasingly important starting from the 1980s [1]. This form of sustainable energy generation is an important contribution for reducing greenhouse gases and achieving the goals of the Kyoto Protocol or the Paris Agreement. The share of total energy used in the building and infrastructure sector is 42 % in the EU ("households" and "commercial and public services" in 2020 [2]), with about two-thirds of energy used in households for heating and cooling [3]. Consequently, the use of geothermal energy for these purposes seems to be highly reasonable, because this form of sustainable energy production is considered to be the most efficient form of building climatization [4]. Due to the current low share of renewable energy sources (23 %) for heating and cooling in the EU [5], there is a large potential for CO_2 savings in this area, especially if renewable primary energy sources are used [6].

In addition, the use of geothermal systems offers the possibility of dual use, i.e., using a single system for both heating and cooling. Due to more efficient thermal insulation and rising air temperatures, the heating demand in Europe is steadily decreasing, while the cooling demand is increasing [7].

Current strongly increasing energy prices as well as a decades long self-created dependence of the European Union (and especially Austria and Germany) on energy supplies from other countries (particularly gas imports from Russia) and the associated problems posed by planning uncertainties and loss of sovereignty [8] are all further arguments for the use of locally sourced geothermal energy.

Apart from energy piles (single piles), energy walls (diaphragm walls or bored pile walls) and energy bottom slabs are now increasingly used. These concrete components are collectively called "energy geostructures" or "thermo-active geostructures" (heat exchangers embedded in earth-coupled concrete structures, and in the majority of cases, foundation elements) and have several advantages over geothermal collectors installed close to the surface or conventional borehole heat exchangers. On the one hand, the corresponding components are needed anyway due to their structural function, which is why the additional costs for equipping them as geothermal heat exchangers are low (synergistic effects). Due to these larger dimensions compared to borehole heat exchangers, thermo-active geostructures meanwhile also result in larger activated volumes (efficiency). Furthermore, the high thermal

conductivity and heat storage capacity of concrete compared to soil or air have a positive effect on energy exchange (thermal properties). Finally, the concrete cover provides excellent protection of the heat exchanger pipes against damage, which means that failures can only occur in the course of installation, these being extremely rare (robustness) [9].

Infrastructure buildings, and thus also metro stations, are particularly suitable for geothermal energy utilization by means of thermo-active geostructures due to the relatively constant energy demand on the one hand (discussed in chapter 2.3) and on the other hand due to the structural components that are necessary anyway in great depths with seasonally constant temperature conditions [9]. In addition, the slightly higher construction costs and at the same time lower operating costs due to the long service life of infrastructure lead to the expectation of a short payback period of the costs. In addition to the economic reasons, however, there are also arguments for the use of geothermal energy in public buildings dealing with social aspects. Such flagship projects can create awareness of energy efficiency and the promotion of sustainable energy sources [10] and thus "set a good example".

In tunnel and thus also in metro construction, energy non-woven geotextiles, energy anchors [1], energy lining segments [11] and energy sheet piles [12] can be used in addition to the systems already mentioned [13–15].

Most projects with energy geostructures have been realized in Austria, the UK, Switzerland and Germany. The technology is also becoming increasingly important in China, although there is only little documented information on the actual extent and functionality of comparable geothermal systems in infrastructure buildings [6].

The Institute of Geotechnics at the TU Wien has been working on the topic of geothermal energy utilization by means of energy geostructures for more than two decades. This concerns basic research [1, 16, 17], numerical modeling [17, 18], application-oriented research [1, 9, 14, 17, 19, 20] and large-scale experiments [21]. The project discussed in this paper was supervised by members of the institute already in the planning phase in the early 2000s, feasibility studies [22, 23] were carried out, the geothermal system was designed, the measurement concept was developed and the installation of the sensors was accompanied [17]. The Institute of Geotechnics at TU Wien is also responsible for the recording and evaluation of both measurement phases, the one from 2008 to 2011 and the one since 2020.

1.2. Scientific relevance and state-of-the-art on the thermo-mechanical behavior of energy walls

While an increasing number of scientific papers on the thermo-mechanical behavior of energy piles based on large-scale tests, laboratory experiments and numerical modeling have been published in the last two decades (a comprehensive listing was made, for example, by Cunha and Bourne-Webb [24]), comparable studies on energy diaphragm walls are hardly available. This circumstance is due to the additional complexity involved combined with less widespread use and a very costly large-scale test execution. Considerations regarding the expansion and deformation behavior of energy diaphragm walls are comparable to those of energy piles (as foundation elements), but in this project they are subject to the following additional complex boundary conditions:

- The bottom slab and (intermediate) ceilings serve as bracing elements and, together with the complete shaft structures with a comparatively complex ground plan geometry, result in a highly statically indeterminate, mutually influencing three-dimensional system in which the stiffness distributions are complex (complex structural geometry).

- Due to the earth and water pressure, the diaphragm walls of the metro station examined here are mainly loaded horizontally and thus as slabs. They bear comparatively small vertical loads as walls due to the lack of a superstructure over the station (complex mechanical loading).

- Due to the large activated area, the temperature load is applied by a large number of heat exchanger circuits, whereby information on the flow rates and temperature distributions is unknown or is only known at certain points. In addition, the wall elements are usually only surrounded by the ground on both sides in the lower area (below the bottom slab), while most of the wall features a ground and air side with each having different boundary conditions (complex thermal loading).

- Individual wall elements (unlike individual piles) cannot be considered decoupled even with otherwise known boundary conditions, since the system deforms as a whole despite a possibly locally limited temperature change (complex thermo-mechanical coupling).

Due to the aforementioned challenges, the studies on energy walls documented in the literature mostly rely on numerical modeling, with possible validation by sparsely available measurement data (see, for example, [25–28]). Results indicate that the air side (and associated heat transfer mechanism by convection) present in energy walls, as opposed to energy piles (as a foundation element), has a strong impact on system performance [26]. This can be advantageous,

but also disadvantageous. For example, if station heating occurs due to waste heat generated by trains and passengers, as has been documented for example in London [29], this could result in an additional energy gain [28]. However, if there is no corresponding heating demand (e.g., in the case of pure cooling demand), this heat generation has a negative effect on the temperature level of the heat exchanger elements.

Previous studies have also shown that seasonal air temperature fluctuations have a greater effect on the temperatures of the energy walls than the heat exchanger operation itself [26]. On the other hand, energy diaphragm walls, for example in Sterpi et al. [30], are attested to have quite relevant additional normal forces and bending moments as a result of thermal operation on the basis of numerical investigations, and which would have to be taken into account in the design.

In order to validate the findings of numerical models on energy walls or energy bottom slabs for infrastructures, actual measurement data are indispensable. While Bourne-Webb et al. in 2016 [26] cite examples of projects with energy diaphragm walls or energy bored pile walls from Austria, the UK, Germany, and China, the authors refer to the data published by Markiewicz [17] and respectively Brandl [1] from the Lainzer Tunnel project (LT24) in Vienna of TU Wien as the only publicly available source of thermo-mechanical measurement data for these wall elements.

In addition to the Lainzer Tunnel, the U2-Taborstraße metro station represents the second infrastructure monitored by TU Wien in which long-term data on the thermo-mechanical behavior of energy walls have been documented. In the course of the world's first large-scale application of thermo-active geostructures in metro stations [1], an energy diaphragm wall element of the Taborstraße station was equipped with numerous measuring instruments. The project has already been presented in [1, 6, 9, 14, 17], among others. To date, however, only temperature data have been published by Brandl et al. [31] in 2010, but no strain or deformation data (Loveridge considers these in [32], but this report has not been published). In the present paper, the investigation of the long-term behavior of a thermo-active energy diaphragm wall is resumed after a decade. A first overview of the continued measurements of temperatures and strains is given, and they are of great importance for the verification of future analytical and numerical theoretical research.

2. Taborstrasse metro station

2.1. Project development of the geothermal plant

In 2001 and 2002 respectively, the builder and operator of the Vienna public transport network, Wiener Linien GmbH & Co KG, commissioned the Institute of Geotechnics of TU Wien, which at that time had already been involved in the research and development of geothermal systems, to prepare technical feasibility studies for geothermal systems [22, 23]. Four of the new metro stations of the U2 line to be extended at that time – U2/1 Schottenring, U2/2 Taborstraße, U2/3 Praterstern and U2/4 Messe-Prater – were then selected with the aim of covering their future heating and cooling needs largely with geothermal energy.

The entire Taborstraße station consists of two shaft structures and two tunnel tubes connected by cross passages. The station building was constructed using the top-down method, with the Taborstraße shaft energy diaphragm walls constructed in 2003 and the energy bottom slab constructed in 2004. Additionally, heat exchanger pipes were also installed in parts of the station tunnel inverts [31].

Figure 1 shows photos of the construction site, with part (a) showing the lower part of the instrumented diaphragm wall (element No. 18) covered with heat exchanger pipes and part (b) showing the installation of this reinforcement cage into the slurry trench. Part (c) shows the connection lines to the energy diaphragm walls as well as one of the three penetration locations through the future 2 m thick bottom slab. Part (d) shows the connection point of heat exchanger circuit No. 2 of diaphragm wall No. 18, the cables of the installed sensors, and the temperature sensors attached to the supply and return lines. The station was opened in May 2008. Figure 2a shows the ground plan of the shaft structure. The respective positions of the two cross sections A-A and B-B, shown in Figure 2b and Figure 2c–d respectively, are indicated in the floor plan (Figure 2a).

The majority of diaphragm wall elements are equipped with two geothermal heat exchanger circuits extending over the entire element height. Those elements that were penetrated by either the tunnels or the staircase are only partially equipped.

The connection of a total of over one hundred heat exchanger circuits [33] to the individual diaphragm wall elements is made below the bottom slab (see Figure 1c and d), which is also fully thermally activated. The design principle followed was to limit the length of the individual heat exchanger circuits, on the one hand, to limit pipe friction losses and, on the other hand, to install them at approximately the same length to ensure largely uniform flow behavior [20].

The quite critical penetration of the heat exchanger circuits into the interior of the structure [20] due to the high groundwater pressure takes place through the base slab at three points, where the distributors T1 to T3 are ultimately also arranged. Subsequently, collector pipes lead to two heat pumps and two cooling machines respectively. The heat exchanger pipes in the thermo-active geostructures, as well as the connecting pipes to the distributors together with the manifolds, form the so-called primary circuit [34].
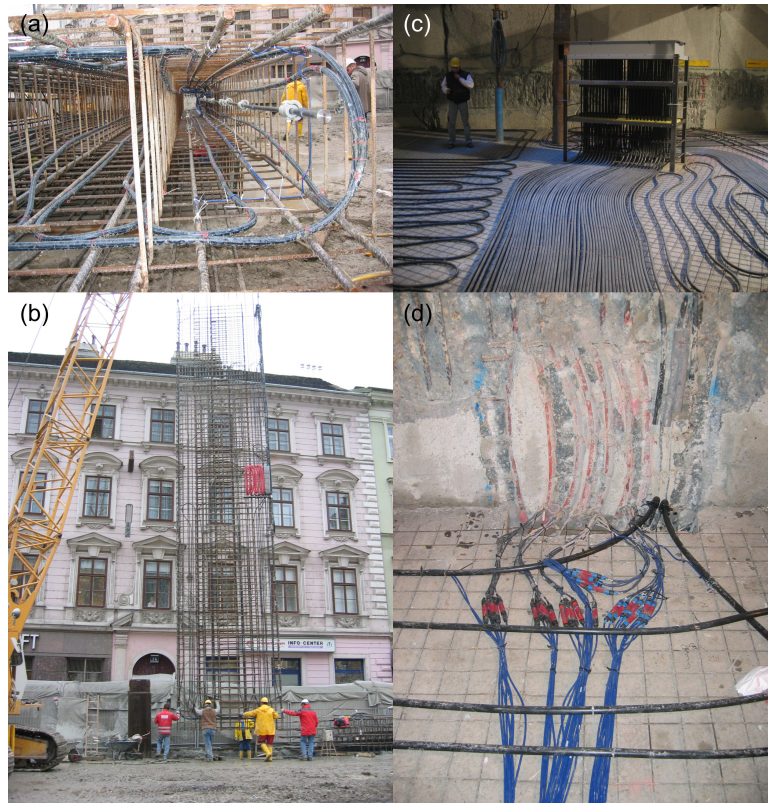
Figure 1. (a) Lower part of the reinforcement cage of the instrumented energy diaphragm wall element No. 18. The sensors were installed on the side to leave the middle chamber free for the contractor tube to avoid damage. (b) Lifting of the lower part of the reinforcement cage of the instrumented energy diaphragm wall element No. 18. The connection point of the heat exchanger pipes and sensor cables under the bottom slab is located at the gray and red protective covers. (c) Heat exchanger pipes below the 2 m thick bottom slab and one of the three feed-through locations into the interior of the structure. (d) Inlet and outlet of heat exchanger circuit No. 2 of the energy diaphragm wall No. 18 as well as the sensor cables (below the bottom slab) and temperature sensors attached to the inlet and outlet pipes.

2.2. Predicted energy demand (design phase)

In a feasibility study [22], various systems for geothermal energy utilization were investigated at an early design stage in order to be able to discover the heating and cooling requirements of the station monitoring rooms, transformer and switch rooms, storerooms, etc. In the course of the execution design, more detailed considerations were given to the selection of thermally usable components, the arrangement of the distribution locations, and the relevant pipe routing. Finally, energy diaphragm walls with a developed area of $2\,300\,\mathrm{m}^2$ and an energy bottom slab with an activated area of $1\,700\,\mathrm{m}^2$ were realized at the U2 station Taborstraße. In addition, an area of $281\,\mathrm{m}^2$ was thermally activated by energy piles and parts of the station tunnels were also equipped with heat exchangers in the invert area [31]. A total of 108 heat exchanger circuits with a total length of $26\,431\,\mathrm{m}$ were installed.

The entire system was designed for the following heating and cooling demands [17]:

- Annual heating energy $175\,\mathrm{MWh\,a}^{-1}$

- Annual cooling energy $437\,\mathrm{MWh\,a}^{-1}$

These numbers represent the usable energy quantities in each case. The heat exchanger load decreases for heating and increases for cooling by their share of electrical energy, as will be described in Chapter 2.3.

Finally, it should be mentioned that the feasibility study also examined the provision of energy for neighboring buildings, but this was not in the end actually implemented.

2.3. Measured energy data (operational phase)

Between October 2008 and July 2010, the energy data of the system was recorded on the first day of each month [36], and since December 2020, approximately monthly. This data is shown in Figure 3 based on the heating and cooling energy used in the secondary circuit, i.e., after the heat pumps and cooling machines respectively. In addition, the electrical energy required to operate the heat pumps, cooling machines, and circulators is also shown.

Figure 3 shows that the heating energy used exceeds the cooling energy by a factor of about 2. However, the external electrical energy supplied to the heat
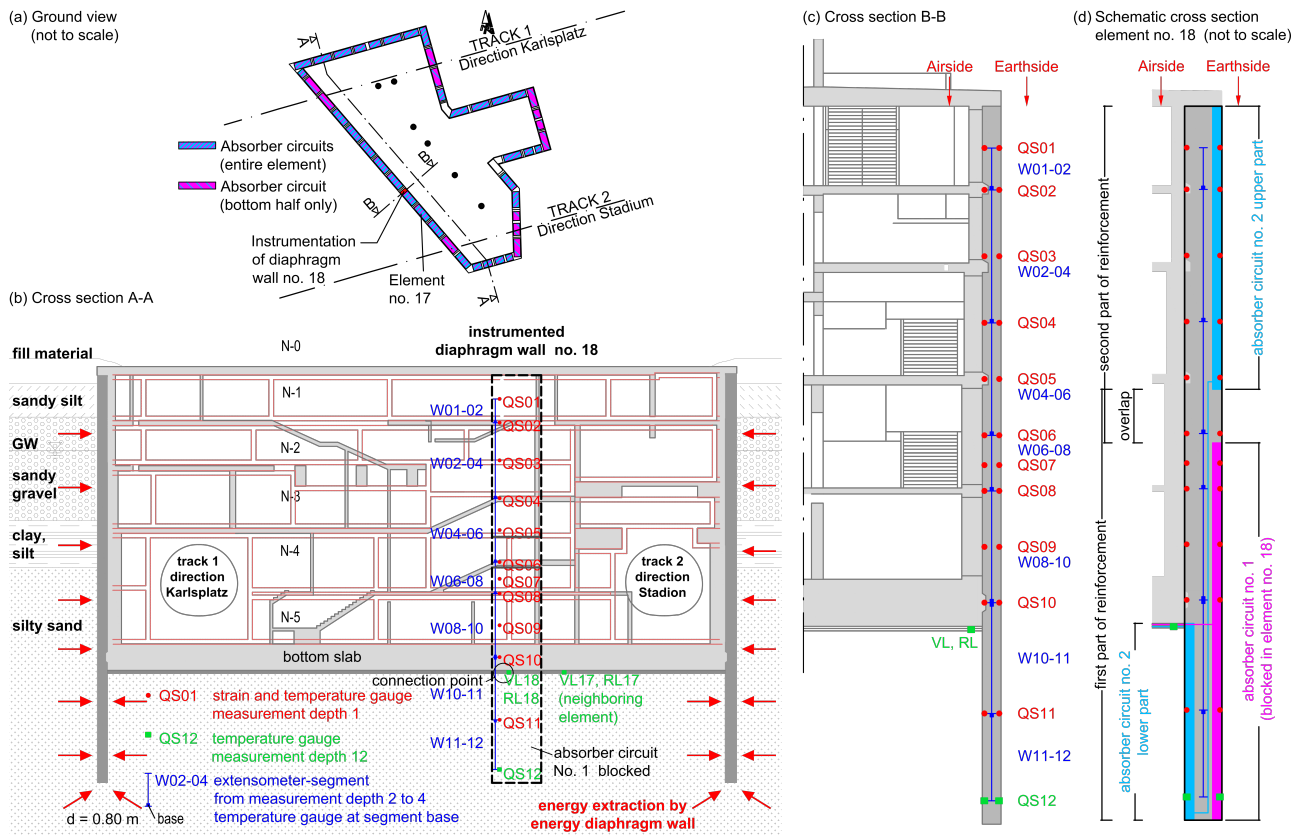
FIGURE 2. (a) Ground view of the metro station Taborstraße section T with position of instrumented diaphragm wall No. 18, neighboring element No. 17 and marked cross sections A-A and B-B. (b) Cross section A-A of U2 metro station Taborstraße section T with ground profile, position of instrumented diaphragm wall No. 18. (c) Cross section B-B of U2 Taborstraße section T, position of instrumented diaphragm wall No. 18 and installed instrumentation. (d) Schematic illustration of the installed heat exchanger circuit's positions (No. 18).
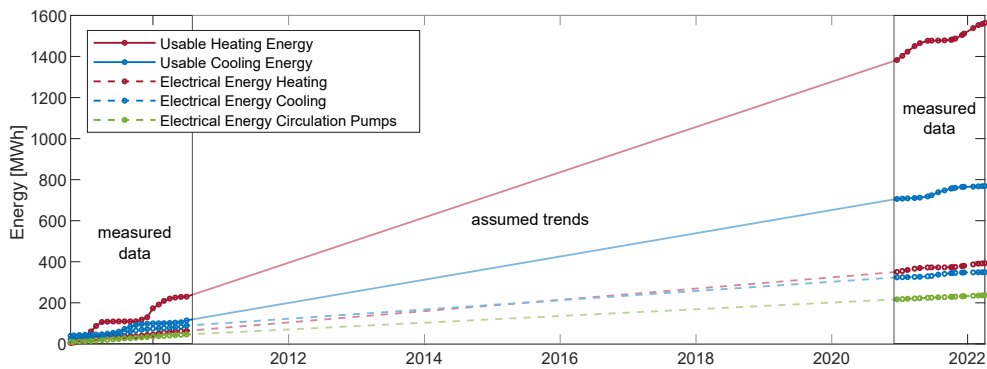

FIGURE 3. Used heating and cooling energy (secondary circle) and external electric energy for heat pumps, cooling machines, and circulation pumps. Measured data from October 2008 to July 2010 and ongoing since December 2020.

pumps or cooling machines is about the same. This is due to the fact that the shares of the required external energy influence the energy actually used in the secondary circuit (on the user side), as shown in Figure 4. Consequently, in the primary circuit, the heat exchanger load is reduced in the heating demand, while the load is increased in the cooling mode. If there is both heating and cooling demand at the same time, the actual heat exchanger load results from the difference between the heating and cooling energy [17].

In this project, the existing energy measurement data can be compared with the predicted energy quantities, as shown in Figure 5. In addition to the predicted monthly energy demand from the design phase [17], the actually measured heating and cooling energy as well as the air temperatures of the Vienna city center [35] are all shown. Since the heating and cooling energy measurements resumed in December 2020 are taken on different days of the month, these measured data are attributed to the individual months
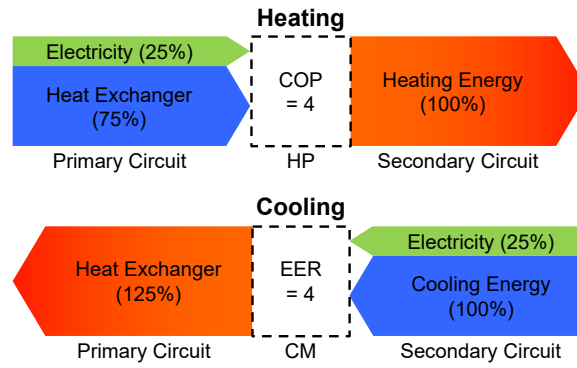
FIGURE 4. Schematic energy flow for heating and cooling. The coefficient of performance COP and energy efficiency ratio EER characterize the efficiency of the heat pumps and cooling machines, respectively.
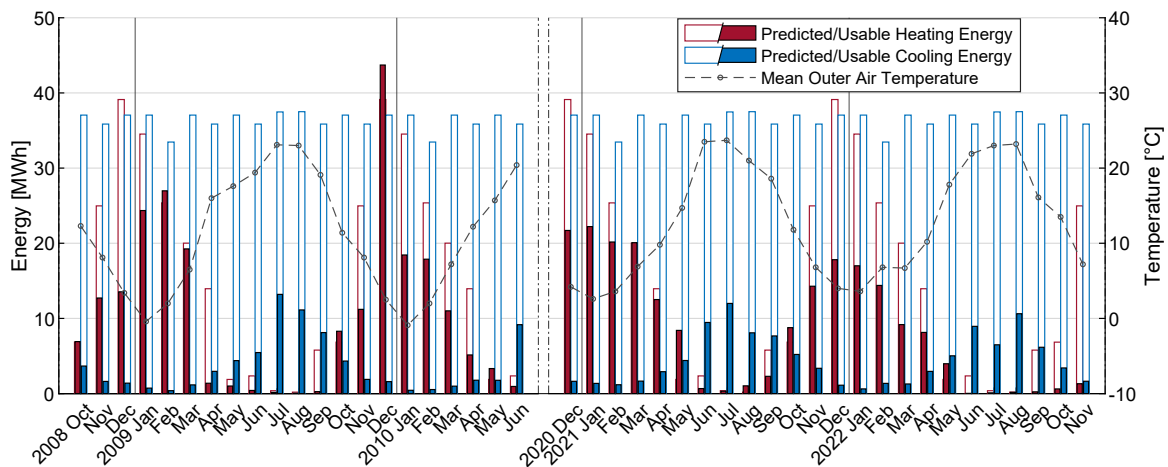

FIGURE 5. Predicted and measured monthly energy totals for heating and cooling, and outer air temperatures of Vienna [35]. The newly collected data since December 2020 is of similar magnitude compared to earlier collected data between 2008 and 2010.

by linear interpolation.

The data collected from December 2020 and onwards are of a similar order of magnitude to those in the first monitoring period from October 2008 to July 2010. Apart from a single peak in heating energy used in December 2009, heating energy reaches monthly peaks between 20 and 27 MWh. Accordingly, the peak consumption of heating energy usually occurs in December or January.

An annual cycle can be chosen as a basis for a comparison of the predicted and measured energy quantities. In this case, for example, the year 2009 is suitable since a complete series of measurements is available. However, it is noticeable that – as already described – in December 2009 a comparatively high amount of used heating energy was recorded compared to the other years. Since the reason for this is unclear (possibly due to the installed staircase heating [34], which was only operated in the first few years), the period December 2008 to November 2009 is chosen as the basis for the following observations.

In the observation period described, the cumulative annual heating energy is 106 MWh. In 2021, i.e., about 10 years later, the cumulative annual heating

energy is 129 MWh. The potential of the thermo-active geostructural system of 175 MWh has thus not yet been exploited, so that there are reserves.

With regard to cooling, the measured data show that in 2009 the annual cooling demand was 55 MWh and in 2021 it was similar at 58 MWh. Compared to the design value of 437 MWh, this shows that there are still larger reserves. In the design phase, a continuous cooling demand over the entire year was assumed. In contrast, however, the measured data show a seasonal fluctuation, with the cooling demand reaching its maximum in July and its minimum in February.

In the design phase, it was also assumed that the cooling demand would increase slowly over the course of the first few years (warming of the structure) and that the design case would only be reached after a few years. However, a comparison of the measured data from the first years with the most recent measured data shows that the cooling demand has not increased significantly since the beginning of monitoring.

In summary, the energy demand can be covered both in the heating case and in the cooling case by means of the installed thermo-active geostructural system for more than 14 years and, in addition, large
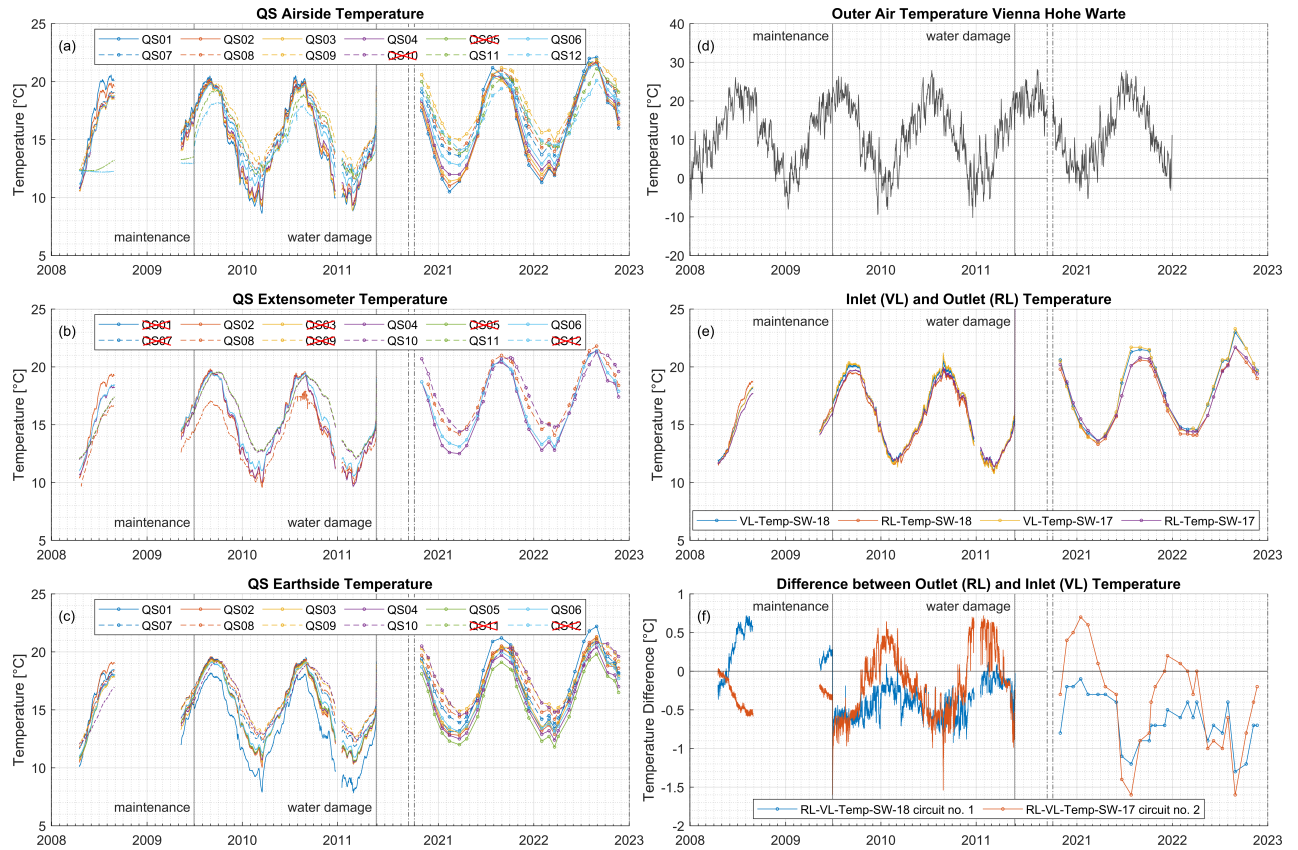
FIGURE 6. Temperature variation with time on the air side (a), center (b) and earth side (c) of the observed diaphragm element. Malfunctioning or not installed sensors are marked by crossed out legend entries. In the center of the element two temperature sensors are placed in QS10 due to the arrangement of the extensometer segments shown in Figure 2d. (d) Air temperature of Vienna, measured at Hohe Warte [36]. (e) Inlet and outlet temperatures of circuit No. 2 of element No. 18 and circuit No. 1 of element No. 17. (f) Differences between outlet and inlet temperatures; a positive value indicates heating operation and a negative vale cooling operation.

reserves are still available, especially in the cooling case.

2.4. INSTRUMENTATION OF THE GEOTHERMAL PLANT

The measurement equipment of the Taborstraße metro station consists of two systems. First, the entire station was equipped with temperature sensors in the diaphragm walls, in the station tubes and under the bottom slab by means of measuring lances [17]. However, due to the high groundwater pressure in combination with unsuitable measuring cables, groundwater was able to penetrate into the measuring center, so that the automatic data acquisition was damaged in 2011 [37].

Second, due to the scientific relevance of this pioneer project, a selected diaphragm wall element (No. 18) was equipped with numerous additional sensors for thermo-mechanical monitoring of the diaphragm wall according to the temperature load. From the associated automatic data acquisition, the measurement data are available from April 2008 until the aforementioned water damage at the end of May 2011 and thus theoretically cover three annual cycles, with a data gap of eight months, as can be seen in Figure 6.

The data generated from October 2020 in the course of the resumed measurements, which are documented selectively at approximately monthly intervals, allow an investigation of the long-term temperature and strain curves of the measuring diaphragm wall. The position of the diaphragm wall element is shown in the design drawing in Figure 2. The additional instrumentation of diaphragm wall element No. 18 includes the following sensors [17]:

- 21 combined temperature and strain transducers (Geokon 4911 Rebar Strainmeters [38]) in the axial direction, each on the air and earth sides.

- One chain extensometer (Geokon 4430 Deformation Meter [39]) consisting of seven segments extending to the base of the diaphragm wall.

- Two temperature sensors (Geokon 3800 thermistor probe [40]) attached to the air and earth sides of the wall base.

- Four temperature sensors (Geokon 3800 thermistor sensors [40]) measuring the inlet and outlet temperatures of the heat exchanger fluid from two circuits.

Figure 2c shows the positioning of the sensors in diaphragm wall element No. 18. Most wall elements at

this station consist of two heat exchanger circuits, as shown in Figure 2d. When the integrity of all heat exchanger circuits was checked during the construction phase, it was found that only three circuits in the entire structure were damaged during construction [31]. However, one of them involved heat exchanger circuit No. 1 of diaphragm wall No. 18 (see Figure 2d). The inlet and outlet temperature gauges intended for this circuit were instead installed on the adjacent element No. 17 (VL17 and RL17).

3. Thermo-mechanical behavior of the diaphragm wall

3.1. Temperature distribution in the diaphragm wall

Figure 6 shows the temperature curve over time for all available sensors on the air side (inside), in the middle and on the earth side (outside) of the diaphragm wall No. 18. As expected, the short-term variation due to the air temperature influence is larger on the air side than on the earth side and decreases with increasing depth. Examination of the earth-side temperatures shows that the largest fluctuations for both the annual and short-term trends occur at the sensors closest to the ground surface.

Knowledge of the layout of the heat exchanger pipes within the diaphragm wall is essential for further interpretation of the temperature measurement data, especially since heat exchanger circuit No. 1 has failed and only heat exchanger circuit No. 2 is intact. In addition, it should be noted that heat exchanger circuit No. 2 runs below the bottom slab on the air side of the diaphragm wall between QS10 and the base of the diaphragm wall and above the bottom slab on the earth side between the top of the diaphragm wall and QS05 (see Figure 2d for details).

Based on Figure 6, it can be seen that the two lowest sensors QS11 and QS12 on the air side well below the bottom slab, where heat exchanger circuit No. 2 runs, show an almost constant temperature curve until the end of June 2009. As it turned out later, this was due to the fact that during this period there was no flow through heat exchanger circuit No. 2 and thus no heat exchanger operation took place in the entire diaphragm wall No. 18. Finally, at the end of June 2009, maintenance work was carried out to check and de-aerate all heat exchanger circuits, and air inclusions were found in a total of 63 % of all circuits [33]. This was also reflected in the temperature measurement data: the temperature level of about 13 °C at the two temperature sensors QS11 and QS12 mentioned above before this maintenance date, thus corresponds in terms of magnitude to the unaffected ground temperature below the bottom slab at depths of 25 m and below, since no energy operation took place in this area. After de-aerating all heat exchanger circuits in June 2009, an energy exchange also took place by means of heat exchanger circuit No. 2, which

can be clearly seen from the measured temperature curve on the air side in cross sections QS11 and QS12. The temperature measurement data on the earth side or in the center of the element do not provide any information on the undisturbed ground temperature, since the temperature sensors located there failed in QS11 and QS12.

For the further interpretation of the temperature measurement data, it proved to be favorable that the mentioned heat exchanger circuit No. 2 was not subject to flow through until June 2009, because of this the entire diaphragm wall element did not participate in the heat exchanger operation, and consequently all measured temperature curves (except those below the ground plate in QS11 and QS12 on the air side) can be attributed to the influence of the air temperature inside the station building. It is noteworthy that the air temperature influences not only the diaphragm wall temperature on the air side, but also those in the middle up to the earth side, and not only in the area of the basement floors, but up to QS10, which is situated in the area of the bottom slab.

After de-aerating heat exchanger circuit No. 2, the diaphragm wall element No. 18 also participated in the heat exchanger operation, whereby it must be noted once again that only partial areas of the diaphragm wall element No. 18 were thermally activated with heat exchanger circuit No. 2. In general, a clear seasonal temperature curve can be seen for all measuring sensors. Since, as will be shown in Figure 6d–f, the flow and return temperatures of heat exchanger circuit No. 2 indicate a similar seasonal variation as with the air temperature, the measured diaphragm wall temperatures can no longer be clearly assigned to the influence of the air temperature or the influence of the heat exchanger operation. In conclusion, it can be assumed that these two influences overlap and that the measured temperatures represent the result of both influences.

The most recent (monthly) readings from October 2020 show a similar annual cyclical pattern as in the first measurement period from April 2008 to May 2011. However, a general temperature increase can be observed within the 10-year observation period. The largest temperature change has occurred at QS01 on the earth side; while in winter 2010 and 2011 the temperature was around 8 °C, this was around 13 °C in winter 2021 and 2022 respectively. However, it is important to note for this data and all data discussed below, that due to the monthly measurement dates in the last observation period, it is not possible to say whether or not the recorded point-by-point data are temporary peaks.

Figure 6d shows the outdoor air temperature of the Hohe Warte measuring station in Vienna [35]. This should serve as an indication of the prevailing climatic conditions for further assessment, since it determines, among other things, the heating and cooling demands and subsequently the required heat exchanger oper-

ation. In addition, the outside air temperature also influences the air temperature inside the station, since a direct exchange of air takes place as a result of the open metro station entrances. Due to the location of the diaphragm wall in the area of such a station access, there is thus also a direct influence on the diaphragm wall temperature.

Depending on the respective heating and cooling demand, a certain flow temperature to the heat exchangers results as a consequence of the system control and the operation of the heat pump or cooling machine. Temperature sensors were installed on the heat exchanger pipes immediately before they were integrated into the diaphragm wall to monitor the flow temperature (see Figure 1d) with the following background: The heat exchanger circuit consists, on the one hand, of connecting pipes running below the bottom slab between the manifold and the diaphragm wall and, on the other hand, of the heat exchanger pipes inside the diaphragm wall, so that an energy exchange with the environment takes place below the bottom slab and inside the diaphragm wall. Sensors for recording the flow and return temperatures were installed on the heat exchanger lines directly in front of the diaphragm wall in order to differentiate these effects. In the case of the diaphragm wall No. 18, where only heat exchanger circuit No. 2 is intact, the flow and return temperatures of this circuit are measured. The supply and return temperatures of this circuit are observed at the adjacent diaphragm wall element (No. 17) in order to obtain information about the energy exchange of heat exchanger circuit No. 1 as well. These measured temperature data are shown in Figure 6d. As mentioned earlier, the temperature curves again show a pronounced seasonal variation. The respective temperature differences are given in Figure 6f in order to assess the energy exchange of the individual heat exchanger circuits. A negative value represents a transfer of energy from the heat exchanger fluid to the ground or environment, i.e., a cooling of the station. Conversely, a positive temperature difference means that an energy extraction and thus a heating operation has taken place. The finding that in the diaphragm wall element No. 18 the heat exchanger circuit No. 2 was blocked at the beginning is also reflected on the basis of Figure 6f, since an opposite trend can be seen until the time of de-aerating in June 2009. After de-aeration has occurred, the two heat exchanger circuits (circuit No. 2 in diaphragm wall element No. 18 and circuit No. 1 in the adjacent diaphragm wall element No. 17, respectively) show a similar seasonal trend in temperature differences, with the absolute temperature difference, and thus the energy exchange, generally being very small (less than 1 °C). For a higher energy exchange, the flow temperature would have to be lower in the heating case and higher in the cooling case, or would have to be specified by the heat pump/cooling machine – however, this is obviously not necessary in the case at

hand, since the heating and cooling demand was or is covered even with this low temperature difference. In conclusion, this also shows that the overall system still has large system reserves.

Furthermore, it is noticeable from Figure 6d that in heating mode an energy exchange only takes place in heat exchanger circuit No. 1 in diaphragm wall element No. 17. In the case of heat exchanger circuit No. 2 in diaphragm wall element No. 18, the flow temperature is apparently higher than the ambient temperature, so that no energy extraction takes place. It should be emphasized that this finding applies only to the monitored diaphragm wall and not necessarily to all other energy diaphragm walls in the station, since the diaphragm wall element No. 18 is significantly influenced by the air temperature due to its location (area of the staircase and station access), and a different interaction with the environment takes place in the case of the other energy diaphragm walls.

Figure 6d–f again shows the long-term trend within the monitoring period of about 10 years. As already observed in the temperature trends based on Figure 6, Figure 6e also shows a certain temperature increase between the initial years from 2008 to 2011 and the most recent monitoring from 2020 onwards. The temperature differences in Figure 6f have remained at a similar order of magnitude, although the temperature difference in cooling mode appears somewhat higher.

3.2. Longitudinal strains of the diaphragm wall

As described in chapter 2.4, the longitudinal strains are measured with strain transducers of the type Geokon 4911 Rebar Strainmeters [38] (so-called "Sister Bars"). These essentially consist of a measuring cell (steel cylinder) with an integrated rebar, which served to attach to the defined cross-sections on the air and earth sides of the rebar cage of the measuring diaphragm wall. When installed or embedded in concrete, the measuring cell thus measures the strains of the rebar and thus of the surrounding reinforced concrete.

The strain measurements are carried out according to the "vibrating wire" principle. In this process, the steel wire present in the measuring cell is set in vibration and the vibration frequency is measured, which depends on the strain of the steel wire. The result of a measurement is output as a so-called "reading" (R). If two measurements (R_0, R_1) are available at two points in time (t_0, t_1), the strain that occurred at the measurement point between the measurement points can be calculated by a calibration factor C specified by the manufacturer:

$$\varepsilon_{\text{Reading}} = (R_1 - R_0)\,C. \qquad (1)$$

Equation (1) must be corrected by a temperature factor in case the temperatures of the measurement cross-section differ at the measurement times (t_0, t_1).
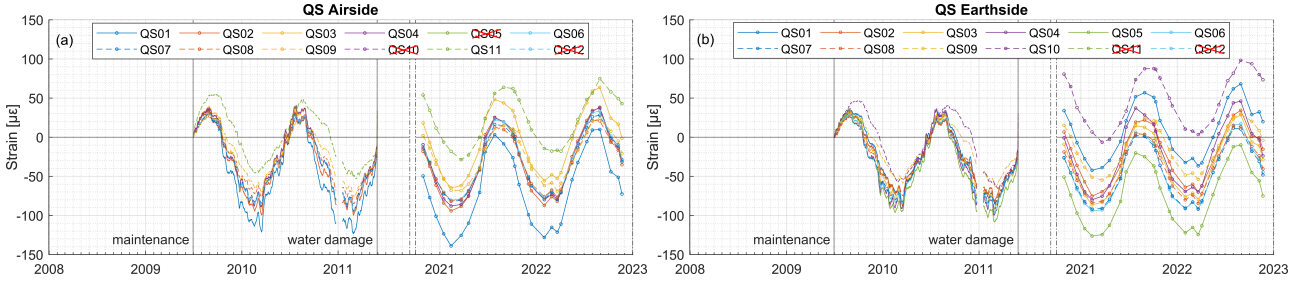
FIGURE 7. Measured strains $\varepsilon_{\mathrm{Obs}}$ (related to datum 2009-07-01) on the air side (a) and earth side (b), in axial direction in various depths (QS01 to QS12). Malfunctioning or not installed sensors are marked by crossed out legend entries.

The reason for this is that the measuring cell is connected to the surrounding reinforced concrete via the rebar and the strain of the measuring cell is always the same as that of the reinforced concrete. However, the steel wire present in the measuring cell does not have a bond with the surrounding structural member and expands more, for example, when the temperature increases due to its larger coefficient of thermal expansion ($\alpha_s \approx 12.2\,\mu\epsilon\,^\circ\mathrm{C}^{-1}$) compared to the reinforced concrete ($\alpha_s \approx 12.2\,\mu\epsilon\,^\circ\mathrm{C}^{-1}$). As a result, the vibrating wire relaxes, which means that the measured value no longer corresponds to the strain of the surrounding reinforced concrete. To account for this in the evaluation, temperature compensation is usually performed as follows.

$$\varepsilon_\sigma = (R_1 - R_0)\,C + \Delta T\,(\alpha_s - \alpha_c). \qquad (2)$$

The strain fraction given in Equation (2) also corresponds to the "load-related strains" $\varepsilon_{\mathrm{load\text{-}related}}$ given in the manufacturer's manual [38]. This is that strain fraction which is caused as a result of stress changes in the component. These stress changes can be caused by mechanical load changes as well as by restraint stresses as a result of elongation or compression due to a change in temperature.

For the temperature-induced strain portion that is not prevented, no additional stresses are generated in the component. This "free" portion of the temperature-induced strains of the reinforced concrete is given by:

$$\varepsilon_{\Delta T} = \Delta T\,\alpha_c. \qquad (3)$$

Both strain components together are ultimately referred to as the "observed" strain $\varepsilon_{\mathrm{Obs}}$ ("observed strain"), since this strain could also be measured with a strain gauge on the component. Consequently, the "observed" strain $\varepsilon_{\mathrm{Obs}}$ results from the two strain components ε_0 and $\varepsilon_{\Delta T}$ to:

$$\varepsilon_{\mathrm{Obs}} = \varepsilon_0 + \varepsilon_{\Delta T}. \qquad (4)$$

If the equations of the corresponding strain components, Equation (2) and Equation (3), are substituted into Equation (4), it simplifies to:

$$\varepsilon_{\mathrm{Obs}} = (R_1 - R_0)\,C + \Delta T\,(\alpha_s - \alpha_c) + \Delta T \cdot \alpha_c,$$
$$\varepsilon_{\mathrm{Obs}} = (R_1 - R_0)\,C + \Delta T\,\alpha_s. \qquad (5)$$

The observed strains $\varepsilon_{\mathrm{Obs}}$ thus also correspond to the strain $\varepsilon_{\mathrm{actual}}$ ("actual strain") stated in the manufacturer's manual [38].

The observed strains $\varepsilon_{\mathrm{Obs}}$ are discussed below and shown in Figure 7. For the interpretation of the measured strains, the choice of the described reference time (t_0 with R_0, T_0) is essential. In this paper, the focus is placed on the representation of the influence of the heat exchanger operation on the diaphragm wall. For the following illustrations, July 1, 2009 is therefore chosen as the reference time, since at this time the metro station building had already been completed and in operation for over a year and it can therefore be assumed that construction-related load and temperature influences had already subsided. Furthermore, no significant static load changes (due to variable traffic loads, earth pressure redistributions, etc.) are to be expected during the operating phase. The existing measurement data between April 16, 2008 and July 1, 2009 are not taken into account, because until the de-aeration of all heat exchanger circuits at the end of June 2009, the intact heat exchanger circuit No. 2 in the diaphragm wall No. 18 was blocked, as already described in chapter 3.1.

Under the aforementioned conditions, all expansions after July 1, 2009 are theoretically due to temperature changes; in this case, they result from the heat exchanger operation on the one hand and from the influence of the air temperature on the other hand. A differentiation in this respect is hardly possible, in particular due to the similar temperature course of the heat exchangers and the air (see Figure 6).

In the strain curves shown in Figure 7, it can be seen in the period from July 2009 to May 2011 that the strains on the air side show a somewhat larger scatter than on the earth side, which is probably due to the influence of the air temperature. Globally, a pronounced seasonal strain pattern is again evident at all monitoring sites, with values varying between approximately $\varepsilon_{\mathrm{Obs}} = 50\,\mu\varepsilon$ (longitudinal strain) and $\varepsilon_{\mathrm{Obs}} = 120\,\mu\varepsilon$ (longitudinal compression). The absolute strain differences in the individual measurement

points, over the year, are $\Delta\varepsilon_{\mathrm{Obs}} = 170\,\mu\varepsilon$ and thus $0.17\,\mathrm{mm\,m}^{-1}$.

About 10 years later, in the monitoring period from October 2020 to April 2022, the measured strains basically show a similar characteristic, i.e., still a pronounced seasonal variation. A detailed analysis shows that on the air side in almost all cross sections the strains are in the same fluctuation range as about 10 years ago. Only in the case of QS1 have somewhat larger compressions occurred. On the earth side, the strains in almost all cross-sections are in the same range of variation as 10 years ago, with somewhat larger compressions occurring in QS05 and somewhat larger strains in QS10.

As already mentioned, it is hardly possible – due to the similar temperature conditions – to assign the strains to the heat exchanger operation or the influence of the air temperature. In addition, it must be taken into account that long-term effects (e.g., creep and shrinkage of the concrete) also have an impact on the measured strains.

In conclusion, however, it is essential that the measurements show that the heat exchanger operation over a longer period of time did not lead to any significant strain changes in the energy diaphragm wall.

4. Summary and outlook

4.1. Summary

Although thermally utilized diaphragm walls and bored pile walls have been increasingly used in recent years, few scientific studies exist on their thermo-mechanical behavior as compared to energy piles. This is due to the complex boundary conditions and the fact that large-scale field tests are very costly. However, the use of these thermo-active geostructures for heating and cooling buildings has enormous potential as a locally obtained and used renewable primary energy source. The Wiener Linien GmbH & Co KG have done international pioneer work with their decision in the early 2000s to supply several metro stations with geothermal energy and to use the structural concrete components, which were necessary anyway for the station structure, as geothermal heat exchangers to cover the heating and cooling demand. Due to the scientific support of the Institute of Geotechnics of TU Wien and the first instrumentation of a thermally activated diaphragm wall element, it has been possible to generate hitherto unique long-term measurement data of the temperature and strain curve of an energy diaphragm wall.

This paper highlights the scientific relevance of the existing and ongoing measurement data of the instrumented energy diaphragm wall in the U2 station Taborstraße. It gives an overview of the project development of geothermal usage at the station and it contains a first presentation and interpretation of the existing measurement data.

Energy data collected since December 2020 in the form of heating and cooling energy used for the entire station show a relatively unchanged energy demand over the entire year compared to the energy demand of the years 2008 to 2010 after the opening of the station. While the prognosis of average annual heating energy carried out in the design phase is almost fulfilled, the actual annual cooling energy required is far lower. Thus, there are still large system reserves, especially for the cooling operation.

The temperature data of the instrumented energy diaphragm wall show a certain increase of the diaphragm wall temperature especially on the earth side and at a shallow depth since the station opening in 2008.

The temperature difference of the heat exchanger fluid between the flow and return is small. This indicates low energy exchange in the observed energy diaphragm wall, which in turn indicates that sufficiently large reserves exist for higher energy extraction or input.

With respect to the selected reference time (July 2009), the strain data of the instrumented energy diaphragm wall show a clear seasonal pattern, which can be attributed to the influence of the air temperature inside the station and the heat exchanger operation. The absolute strain difference between winter and summer is a maximum of $\Delta\varepsilon_{\mathrm{Obs}} = 170\,\mu\varepsilon$ and thus $0.17\,\mathrm{mm\,m}^{-1}$ for all recorded measurement points. The magnitude of this strain difference did not change over time; only slightly higher strains were observed at individual measurement points.

4.2. Outlook

The currently available temperature and strain data of an energy diaphragm wall element provide a basis for future research with respect to geothermally utilized earth-coupled wall elements. In particular, the thermally induced stresses from seasonal air temperature fluctuations and a heating and cooling operation are of great interest for researching thermo-mechanical component behavior. The measured data generated in this process provide a verification basis for mechanical and numerical models.

The current measurements will be continued and thus allow continuous extension of the data series. In addition, temperature sensors were installed at one of the three distributors in the fall of 2021 to record supply and return temperatures and to analyze the behavior of the system in more detail.

Furthermore, the geothermal system of the metro station with the usable heating and cooling energy that results, offers insights for any dimensioning or assessment of similar systems in the future.

4.3. Final remark

The contents of this article have already been published in German as an original paper for the renowned journal Bauingenieur [41].

REFERENCES

[1] H. Brandl. Energy foundations and other thermo-active ground structures. *Géotechnique* **56**(2):81–122, 2006. https://doi.org/10.1680/geot.2006.56.2.81

[2] Eurostat. Final energy consumption by sector, 2022. [2022-04-06]. https://ec.europa.eu/eurostat/databrowser/view/TEN00124__custom_2439979/default/table?lang=en.

[3] Eurostat. Energy consumption in households, 2022. [2022-04-06]. https://ec.europa.eu/eurostat/statistics-explained/index.php?title=Energy_consumption_in_households#Energy_consumption_in_households_by_type_of_end-use.

[4] S. Yoon, S.-R. Lee, G.-H. Go. Evaluation of thermal efficiency in different types of horizontal ground heat exchangers. *Energy and Buildings* **105**:100–105, 2015. https://doi.org/10.1016/j.enbuild.2015.07.054

[5] Eurostat. Share of renewable energy in gross final energy consumption by sector, 2022. [2022-04-06]. https://ec.europa.eu/eurostat/databrowser/view/sdg_07_40/default/table?lang=en.

[6] L. Laloui, A. F. R. Loria. *Analysis and design of energy geostructures: theoretical essentials and practical application.* Academic Press, 2020. ISBN 978-0-12-820623-2.

[7] Eurostat. Heating of buildings decreasing, cooling increasing, 2022. [2022-04-06]. https://ec.europa.eu/eurostat/en/web/products-eurostat-news/-/ddn-20210311-1.

[8] L. Rodríguez-Fernández, A. Carvajal, V. d. Tejada. Improving the concept of energy security in an energy transition environment: Application to the gas sector in the European Union. *The Extractive Industries and Society* **9**:101045, 2022. https://doi.org/10.1016/j.exis.2022.101045

[9] H. Brandl. Geothermal geotechnics for urban undergrounds. *Procedia Engineering* **165**:747–764, 2016. https://doi.org/10.1016/j.proeng.2016.11.773

[10] J. A. Camacho Ballesta, L. da Silva Almeida, M. Rodríguez. An analysis of the main driving factors of renewable energy consumption in the European Union. *Environmental Science and Pollution Research* **29**(23):35110–35123, 2022. https://doi.org/10.1007/s11356-022-18715-z

[11] S. Frodl, J. Franzius, T. Bartl. Design and construction of the tunnel geothermal system in Jenbach. *Geomechanics and Tunnelling* **3**(5):658–668, 2010. https://doi.org/10.1002/geot.201000037

[12] D. Koppmann. *Untersuchung der thermischen Aktivierung von Stahlspundwänden.* Ph.D. thesis, RWTH Aachen, 2021.

[13] D. Adam, R. Markiewicz. Nutzung der Geothermie mittels Erdwärmeabsorber und Grundwasserbrunnen. *Österreichische Wasser- und Abfallwirtschaft* **62**(5):77–85, 2010. https://doi.org/10.1007/s00506-010-0183-4

[14] D. Adam, R. Markiewicz. Energy from earth-coupled structures, foundations, tunnels and sewers. *Géotechnique* **59**(3):229–236, 2009. https://doi.org/10.1680/geot.2009.59.3.229

[15] P. Bourne-Webb, R. Gonçalves. On the exploitation of ground heat using transportation infrastructure. *Procedia Engineering* **143**:1333–1340, 2016. https://doi.org/10.1016/j.proeng.2016.06.157

[16] D. Adam, R. Markiewicz. Nutzung der geothermischen Energie mittels erdberührter Bauwerke: Teil 1: Theoretische Grundlagen. *Österreichische Ingenieur- und Architekten-Zeitschrift (ÖIAZ)* **147**(4):120–138, 2002.

[17] R. Markiewicz. *Numerische und experimentelle Untersuchungen zur Nutzung von geothermischer Energie mittels erdberührter Bauteile und Neuentwicklungen für den Tunnelbau.* Ph.D. thesis, TU Wien, 2004.

[18] D. Adam, R. Markiewicz. Nutzung der geothermischen Energie mittels erdberührter Bauwerke – Teil 2: Experimentelle Untersuchungen und Computersimulationen. *Österreichische Ingenieur- und Architekten-Zeitschrift (ÖIAZ)* **147**(5-6):162–170, 2002.

[19] D. Adam, R. Markiewicz. Nutzung der geothermischen Energie mittels erdberührter Bauwerke – Teil 3: Ausführungsbeispiele und Neuentwicklungen. *Österreichische Ingenieur- und Architekten-Zeitschrift (ÖIAZ)* **148**(1), 2003.

[20] Österreichische Bautechnik Vereinigung. Richtlinie: Erdwärmenutzung mit Massivabsorbern. Österreichische Bautechnik Vereinigung, 2019.

[21] R. Markiewicz, D. Adam. *Forschungsprojekt Unteres Hausfeld – Teil 3 – Energiepfahlversuche.* Institut für Geotechnik TU Wien, Wien, 2020.

[22] TU Wien. Planungsgemeinschaft U2/2 Taborstraße. Machbarkeitsstudie Erdwärmenutzung. Bauabschnitt U2/2 Taborstraße. TU Wien Ausgabe 2001.

[23] TU Wien. iC Consulenten: Machbarkeitsstudie Erdwärmenutzung. Bauabschnitt U2/1 Schottenringstraße, Bauabschnitt U2/2 Taborstraße, Bauabschnitt U2/3 Praterstern, Bauabschnitt U2/4 Messe. TU Wien Ausgabe 2002.

[24] R. Cunha, P. Bourne-Webb. A critical review on the current knowledge of geothermal energy piles to sustainably climatize buildings. *Renewable and Sustainable Energy Reviews* **158**:112072, 2022. https://doi.org/10.1016/j.rser.2022.112072

[25] A. Di Donna, F. Loveridge, M. Piemontese, et al. The role of ground conditions on the heat exchange potential of energy walls. *Geomechanics for Energy and the Environment* **25**:100199, 2021. https://doi.org/10.1016/j.gete.2020.100199

[26] P. Bourne-Webb, T. Bodas Freitas, R. Da Costa Gonçalves. Thermal and mechanical aspects of the response of embedded retaining walls used as shallow geothermal heat exchangers. *Energy*

and Buildings **125**:130–141, 2016.
https://doi.org/10.1016/j.enbuild.2016.04.075

[27] A. Coletto, D. Sterpi. Structural and geotechnical effects of thermal loads in energy walls. *Procedia Engineering* **158**:224–229, 2016.
https://doi.org/10.1016/j.proeng.2016.08.433

[28] A. Di Donna, F. Cecinato, F. Loveridge, et al. Energy performance of diaphragm walls used as heat exchangers. *Proceedings of the Institution of Civil Engineers – Geotechnical Engineering* **170**(3):232–245, 2017. https://doi.org/10.1680/jgeen.16.00092

[29] M. Botelle, K. Payne, B. Redhead. Squeezing the heat out of London's tube. *Proceedings of the Institution of Civil Engineers – Civil Engineering* **163**(3):114–122, 2010. https://doi.org/10.1680/cien.2010.163.3.114

[30] D. Sterpi, A. Coletto, L. Mauri. Investigation on the behaviour of a thermo-active diaphragm wall by thermo-mechanical analyses. *Geomechanics for Energy and the Environment* **9**:1–20, 2017.
https://doi.org/10.1016/j.gete.2016.10.001

[31] H. Brandl, D. Adam, R. Markiewicz, et al. Massivabsorbertechnologie zur Erdwärmenutzung bei der Wiener U-Bahnlinie U2. *Ingenieur- und Architekten-Zeitschrift* **155**(7-9):10–12, 2010.

[32] F. Loveridge. Interpretation of monitoring data at Vienna U2 Taborstrasse station. University of Southampton, 2010.

[33] Enercret. Prüfprotokoll – Baustelle U2/2. Verteiler T1, T2 und T3. Juni 2009.

[34] Wiener Linien Anlagenschema Heizung / Erdwärme / Kälte. Bestandsplan. 2007.

[35] ZAMG. Jahrbuch der klimatologische Tages-, Monats- und Jahresauswertungen der Lufttemperatur für Wien Hohe Warte und Wien Innere Stadt. 2022. [2022-03-21]. https://www.zamg.ac.at/cms/de/klima/klimauebersichten/jahrbuch.

[36] J. Mauritz, S. Sailer, M. Salmhofer, et al. *Ermittlung der Energieeffizienz der Geothermieanlage in der U-Bahnstation U2 Taborstraße.* Master's thesis, HTBLuVA – TGM Höhere Lehranstalt für Berufstätige für Wirtschaftsingenieurwesen, 2010.

[37] Kontrollamt der Stadt Wien. Wiener Linien GmbH & Co KG, Nutzung der Erdwärme. 2011. [2022-04-05]. https://stadtrechnungshof.wien.at/berichte/2011/lang/02-12-KA-V-GU-230-3-11.pdf.

[38] Geokon. Installation Manual. Models 4911/4911A. Vibrating Wire Rebar Strain Meters. 2019. [2021-06-28]. https://www.geokon.com/4911-4911A.

[39] Geokon. Installation Manual. Model 4430. VW Deformation Meter. 2021. [2021-06-28]. https://www.geokon.com/4430.

[40] Geokon. Installation Manual. Model 3800/3810. Thermistors & Thermistor Strings. 2021. [2021-06-28]. https://www.geokon.com/3800.

[41] A. Brunner, R. Markiewicz, J. Pistrol, D. Adam. Langzeiterfahrungen zur geothermischen Nutzung der U-Bahn-Station Taborstraße in Wien. *Bauingenieur* **97**(7-8):248–261, 2022. https://doi.org/10.37544/0005-6650-2022-07-08-68